Am J Nucl Med Mol Imaging 2026;16(5):242-249
www.ajnmmi.us /ISSN:2160-8407/ajnmmi0173317

Original Article

Performance of SPECT myocardial perfusion imaging in fulminant myocarditis: comparison to cardiac magnetic resonance imaging

Yuxin Yang[1,2,3], Shuwen Wang[4], Zhifang Wu[1,2], Yinghui Ge[4], Chengyan Dong[1,2], Jing Cui[3]

[1]Department of Nuclear Medicine, First Hospital of Shanxi Medical University, Taiyuan, Shanxi, China; [2]Molecular Imaging Precision Medical Collaborative Innovation Center, Shanxi Medical University, Taiyuan, Shanxi, China; [3]Department of Nuclear Medicine, Fuwai Central China Cardiovascular Hospital, Zhengzhou, Henan, China; [4]Department of Radiology, Fuwai Central China Cardiovascular Hospital, Zhengzhou, Henan, China

Received April 14, 2026; Accepted October 25, 2026; Epub October 25, 2026; Published October 30, 2026

Abstract: This study investigated SPECT myocardial perfusion imaging (MPI) features in patients with fulminant myocarditis (FM) and evaluated correlations between quantitative MPI parameters and cardiac magnetic resonance (CMR) characteristics. A retrospective analysis was conducted on patients clinically suspected of FM at Fuwai Central China Cardiovascular Hospital who underwent both SPECT MPI and CMR. CMR was quantitatively analyzed including native T1, T2 mapping, extracellular volume (ECV), late gadolinium enhancement (LGE), and left ventricular ejection fraction (LVEF_CMR). MPI was analyzed using the 17-segment model, collecting summed rest score (SRS) and LVEF (EF_MPI). MPI performance in detecting abnormality extent and severity was compared with CMR at global and wall segment level (anterior wall, apex, inferior, septal, and lateral). Among 77 included patients, 77 (100%) had abnormal MPI findings, and 75 (97.4%) had abnormal CMR findings. For 308 ventricular wall segments, 239 (77.6%) showed reduced perfusion on MPI, while 214 (69.5%) were positive on CMR. MPI demonstrated an overall diagnostic agreement rate of 69.8% (215/308) with a positive agreement rate of 84.1% (180/214) and a negative agreement rate of 44.7% (42/94). Quantitative analysis revealed LGE and T2 mapping were negatively correlated with EF_MPI ($P < 0.05$), while Native T1 and ECV were positively correlated with SRS ($P < 0.05$). EF_CMR showed positive correlation with EF_MPI and negative correlation with SRS ($P < 0.01$). By offering more detailed functional imaging information, MPI provides complementary value to CMR in early diagnosis and evaluation of myocardial injury in FM, particularly when CMR is contraindicated or technically challenging.

Keywords: Fulminant myocarditis, myocardial perfusion imaging, cardiac magnetic resonance

Introduction

Fulminant myocarditis (FM) is the most severe and distinct form of myocarditis, characterized by rapid progression, hemodynamic dysfunction and circulation instability, often requiring mechanical circulation support (MCS) [1, 2]. It is a leading cause of cardiogenic shock in young adults [3, 4]. Large-scale multicenter studies show FM accounts for approximately 10% of all myocarditis cases [1, 5]. In China, an estimated 30,000 to 50,000 new adult cases (aged > 14 years) of FM occur annually [6]. Previous research reports that in-hospital mortality can reach as high as 45%-55.6% [7], though Chinese expert team introduced "A life support-based comprehensive treatment regimen" which dramatically reduced this to below 5% [2], emphasizing the prompt and accurate diagnosis at the earliest possible stage.

The pathophysiology of FM includes extensive myocardial inflammation, cardiomyocyte necrosis, interstitial edema and circulatory dysfunction [6]. Endomyocardial biopsy (EMB) is the diagnostic gold standard [6, 8], but its routine use is challenging due to invasiveness and sampling variability. Consequently, imaging plays a vital role in diagnosis, differential diagnosis, evaluation, and follow-up, providing essential information regarding myocardial edema, fibrosis, perfusion abnormalities, and cardiac structure and function [9].

Cardiac magnetic resonance (CMR) is well-established for diagnosing clinically suspected myocarditis (CSM) [3], offering high-resolution structural imaging and detailed tissue characterization via T1/T2-weighted imaging, late gadolinium enhancement (LGE), and mapping techniques [10, 11]. However, CMR has notable limitations, including long scan times, need for breath-holding, high operator expertise, and limited applicability in hemodynamically unstable patients or those on MCS, making it not always feasible for FM patients [6]. Potential adverse reactions to gadolinium-based contrast agents further restrict its utility during the acute phase.

SPECT myocardial perfusion imaging (MPI) is a widely available, relatively low-cost method for evaluating global and regional myocardial perfusion and left ventricular (LV) function [12]. Nevertheless, its application in myocarditis remains controversial. This study aims to analyze MPI features in FM patients and evaluate correlations between quantitative MPI parameters and CMR characteristics, providing a reference for clinical diagnosis and treatment decisions.

https://doi.org/10.62347/BWKZ1047

Materials and methods

Subjects

This retrospective study enrolled patients clinically diagnosed with FM who underwent both SPECT MPI and CMR during a single hospitalization at Fuwai Central Cardiovascular Hospital from March 2018 to December 2024.

The diagnosis of FM was established by the treating clinical team according to the Chinese Society of Cardiology guidelines [6], based on: 1) Acute onset with rapid progression to severe hemodynamic compromise or life-threatening arrhythmias; significantly elevated cardiac injury markers, including high-sensitivity cardiac troponin I (hs-cTnI) and N-terminal pro-brain natriuretic peptide (NT-proBNP); and distinct electrocardiographic (ECG) changes. 2) Echocardiographic findings showing diffuse ventricular wall motion abnormalities and a marked reduced LV ejection fraction (LVEF). Elevated inflammatory markers such as C-reactive protein (CRP), erythrocyte sedimentation rate (ESR), interleukins, and procalcitonin (PCT) were also observed. Acute myocardial infarction was excluded by coronary angiography or coronary CT angiography, and Takotsubo syndrome, inherited cardiomyopathies, and other specific inflammatory cardiomyopathies were excluded based on clinical presentation, imaging features, and absence of characteristic findings (e.g., apical ballooning, hypertrophic patterns, or specific systemic disease markers) [6]. CMR was performed after weaning from MCS and once hemodynamic stability was achieved.

Clinical data

Clinical information and laboratory test results were collected including: age, gender, New York Heart Association (NYHA) class, high-sensitivity troponin T (hs-cTnT), NT-proBNP, white blood cell (WBC) count, neutrophil count, lymphocyte count, high-sensitivity CRP (hs-CRP), PCT, and ESR.

SPECT MPI acquisition and analysis

Patients consumed a high-fat meal at 30 minutes (min) after intravenous injection of 740 MBq (20 mCi) ^{99m}Tc-MIBI (Zhengzhou Atomic Hi-Tech Co., Ltd., radiochemical purity > 95%), and underwent 5-min rest MPI (8 frames gated-MPI) 90 min post-injection using a digital cardiac-dedicated CZT SPECT system (Discovery NM530c, GE Healthcare). Energy peak was set at 140 keV ± 10%. Data were iteratively reconstructed (Myovation for Alcyon, GE Healthcare).

Images were analyzed on workstation (Xeleris 4DR) using QGS/QPS software (Cedars-Sinai, USA). LVEF (EF_MPI) was automatically quantified. Gated MPI acquisition was not performed in all patients due to the retrospective nature of data collection and variability in clinical protocols during the early study period; EF_MPI was available for 33 of 77 patients. Visual analysis of perfusion defects on five left ventricular wall segment levels (anterior, septal, lateral, inferior, apical) was performed by two experienced senior nuclear medicine physicians. And visual scoring was performed using the 17-segment model to calculate the Summed Rest Score (SRS) on a five-point scale (0 = normal, 1 = mildly reduced, 2 = moderately reduced, 3 = severely reduced, 4 = absent). Discrepancies resolved by consensus.

CMR imaging and analysis

CMR was performed on a 3 T MRI system (MAGNETOM Skyra, Siemens Healthineers, Erlangen, Germany) with an 18-channel cardiac coil and acceleration factor of 2, using respiratory and ECG gating. Sequences included: (1) Cine bright-blood imaging using steady-state free precession (SSFP) sequence (TR: 39.24 ms, TE: 1.43 ms, thickness: 8 mm, gap: 2 mm). (2) Native T1 (MOLLI) (TR 280.6 ms, TE 1.1 ms, FOV 360 × 306 mm, matrix 256 × 144, thickness: 8 mm). (3) T2 mapping (T2-prepared multi-echo GRE) (TR 207.4 ms, TE 1.3 ms, FOV 360 × 288 mm, matrix 192 × 116, thickness: 8 mm). (4) Fat-suppressed T2-weighted imaging (T2WI) (TR: 400 ms, TE: 44 ms, TI: 160 ms, thickness: 6 mm). (5) Resting first-pass perfusion imaging (TR: 165 ms, TE: 0.98 ms, TI: 95 ms, thickness: 8 mm) using gadopentetate dimeglumine (Magnevist, Bayer, Germany) at 0.3 ml/kg. (6) LGE imaging (segmented turbo-FLASH-PSIR) approximately 10 minutes post-contrast (TR: 700 ms, TE: 1.96 ms, TI: 300 ms, adjusted as needed, thickness: 8 mm).

Two experienced radiologists blinded to clinical data performed image analysis using commercial software (CVI42, version 5.14.1, Circle, Calgary, Canada). Native T1 and T2 mapping were acquired on basal, mid-ventricular and apical left ventricular short-axis slices. ROIs were manually drawn along endocardial and epicardial contours, carefully avoiding the blood pool and papillary muscles. Mean values were calculated across all myocardial segments. ECV was calculated from pre- and post-contrast T1 maps and hematocrit. LGE was quantified using the full-width half-maximum method. Cutoff values for abnormality were: native T1 > 1250 ms, T2 > 45 ms, ECV > 26%, and LGE > 5% of myocardial area, based on institutional normal references and published recommendations [11, 13-15].

Statistical analysis

Statistical analysis was performed using SPSS 22.0 software (IBM SPSS Statistics 22.0). Normally distributed continuous data are presented as mean ± standard deviation (x ± s), and are compared between groups using independent samples t-test. Non-normally distributed

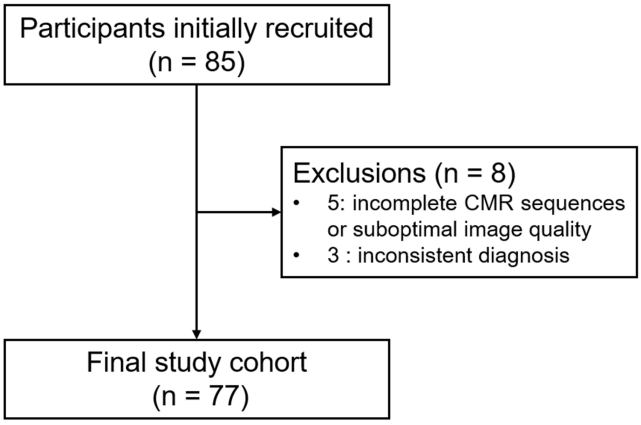


Figure 1. Flowchart of patient inclusion/exclusion.

continuous data are presented as median with interquartile range (Q1, Q3), and are compared using Mann-Whitney U test. Comparison among more than two groups used Kruskal-Wallis test. Categorical data are presented as n (%), and compared using χ^2 test. Correlation analysis between continuous variables used Spearman's correlation. Interobserver reproducibility of visual semiquantitative MPI scores and the agreement between MPI, CMR, and clinical data was assessed using Kappa test. Sensitivity, specificity, positive predictive value (PPV), negative predictive value (NPV), and accuracy with 95% confidence intervals were calculated for MPI against CMR as the reference at both patient and segment levels. A *P*-value < 0.05 was considered statistically significant.

Results

Baseline clinical characteristics

A total of 77 patients were included (**Figure 1**; **Table 1**). During hospitalization, 31 patients (40.3%) received intra-aortic balloon pump (IABP), 25 (32.5%) extracorporeal membrane oxygenation (ECMO), and 13 (16.9%) mechanical ventilation. ECG on admission revealed ST-T segment abnormalities in 64 (83.1%), including ST-elevation in 21 (27.3%). Arrhythmias occurred in 63 (81.8%), with high-grade atrioventricular block in 30 (39.0%). Only 2 (2.6%) had no significant ECG abnormalities. For MPI visual scoring of two reviewers, Cohen's kappa was 0.87 (95% CI: 0.77-0.96).

Imaging results

All the 77 patients (100.0%) were found with perfusion abnormalities on rest MPI. Diffuse hypoperfusion was observed in 18 (23.4%), with involvement of five walls in 23 (29.9%), four walls in 25 (32.4%), three walls in 19 (24.7%), two walls in 9 (11.7%), and a single wall in 1 (1.3%). The median of SRS was 5 (3, 8), range 2-23. Among the 33 patients with gated MPI acquisition, median EF_MPI was 64% (50%, 69%), range 15%-81%.

CMR identified abnormalities in 75 patients (97.4%), including LGE in 71 cases (92.2%), T2 hyperintensity in 40 (51.9%), and reduced first-pass perfusion in 40 (51.9%). Regarding the extent of involvement, positive findings were observed in all four walls in 37 patients (48.1%), three walls in 7 (9.1%), two walls in 14 (18.2%), and a single wall in 17 (22.1%). Median EF_CMR was 53% (42%, 61%). Representative cases are shown in **Figures 2**, **3**, respectively.

Among 308 wall segments (excluding apex), MPI revealed reduced perfusion in 239, while CMR detected positive findings in 214 (**Table 2**). MPI identified reduced radiotracer uptake in the apex in 52 patients.

At the segment level, using CMR as reference, MPI had a sensitivity of 84.1% (95% CI: 78.5-88.6%), specificity of 37.2% (95% CI: 27.8-47.6%), accuracy of 69.8% (95% CI: 64.3-74.8%), PPV of 75.3% (95% CI: 69.4-80.4%), and NPV of 50.7% (95% CI: 39.2-62.2%). At the patient level, MPI sensitivity was 100% (75/75), while specificity was 0% (0/2), although the latter estimate was based on only two CMR-negative patients. Agreement between MPI and CMR parameters yielded kappa values of 0.136 (P < 0.001) for T2 hyperintensity, 0.173 (P < 0.001) for LGE, -0.011 (P < 0.001) for reduced perfusion on CMR, 0.153 (P < 0.01) for all three combined, and 0.194 (P < 0.01) for T2+LGE combined.

Correlations of SRS and EF_MPI with CMR quantitative parameters and laboratory data were listed in **Table 3**. SRS showed significant positive correlations with T1, ECV, NT-proBNP, Lymphocytes, and negative correlation with EF_CMR. EF_MPI showed significant negative correlations with LGE, T2, WBC, Lymphocytes, PCT, and positive correlation with EF_CMR.

Discussion

In this study, both MPI and CMR demonstrated high abnormality detection rates in this cohort of clinically diagnosed FM patients, at 100% and 97.4%, respectively. The diagnosis of FM primarily relies on clinical presentation and exclusion of other causes [6]. CMR serves to validate the clinical diagnosis and assess the inflammation, while MPI reflects reduced perfusion and myocardial injury through abnormal radiotracer distribution. The MPI positive rate was higher than that reported by Yang et al. [16] in clinically suspected myocarditis, likely because FM involves diffuse inflammatory involvement [8], with broader and more severe lesions. Additionally, the use of a cadmium-zinc-telluride (CZT) dedicated cardiac camera offers significantly higher detection efficiency than conventional NaI detectors, improving image quality and diagnostic accuracy [17]. The 100% sensitivity in our study aligns with Liang et al. [18].

Table 1. General characteristics of patients

Variable	Over all (n = 77)
Age (years old, yo)	33 (24, 43)
Gender	
Male	33 (42.9%)
NYHA Functional Class IV/III/II/Not classified	31 (40.3%)/14 (18.2%)/8 (10.4%)/24 (31.2%)
Cardiogenic shock/arrest	39 (50.6%)
Tachypnea	27 (35.1%)
IABP/ECMO/Mechanical ventilation	31 (40.3%)/25 (32.5%)/13 (16.9%)
WBC count (× 10^9/L)	11.64 (10.19, 13.7)
Neutrophil count (× 10^9/L)	9.98 ± 3.88
Lymphocyte count (× 10^9/L)	0.68 (0.52, 0.98)
hs-CRP (mg/L)	22.99 (8.19, 51.07)
NT-proBNP (pg/mL)	1263.50 (525.10, 2590.00)

SPECT MPI is commonly applied in coronary artery disease. ^{99m}Tc-MIBI is rapidly taken up by normal cardiomyocytes and concentrates in mitochondria [19]. In the absence of epicardial coronary artery stenosis (confirmed by angiography), the mechanisms underlying MPI perfusion reduction in FM include [6, 20]: 1) direct or indirect pathogen-induced myocardial degeneration, necrosis, and dysfunction, which prevent effective tracer retention in cardiomyocytes; 2) cytokine release causing inflammatory edema and microenvironmental changes limiting tracer diffusion; 3) inflammation-induced coronary spasm or rare coronary thrombosis impairing tracer perfusion. Furthermore, increased expression of adhesion molecules in coronary intramural vascular endothelial cells suggests that inflammation may reduce coronary perfusion reserve [16, 21]. FM-induced mitochondrial dysfunction causes multifocal perfusion abnormalities not matching coronary territories, helping differentiate FM from coronary artery disease-related defects. In our study, 71.4% (55/77) of patients exhibited perfusion abnormalities involving three or more wall segments, and even in the remaining 21 patients, no matching with coronary territories was observed.

SPECT MPI may provide complementary information on myocardial injury in patients with myocarditis. Perfusion defects on SPECT MPI have been reported in myocarditis from various causes, like different infection sources [16, 22, 23], systemic lupus erythematosus [24] and immune checkpoint inhibitor myocarditis [25].

In CMR, increased myocardial water content prolongs myocardial T2 relaxation time, with edema appearing as focal or diffuse hyperintensity on T2-weighted imaging and quantitative T2 mapping. Early gadolinium enhancement reflects tissue hyperemia, increased vascular permeability, and extracellular expansion. LGE becomes more pronounced with necrosis, fibrosis, or scar. Mapping techniques enable quantitative T1/T2 measurement. ECV calculated from pre/post-contrast T1 and hematocrit overcomes limitations of visual or semi-quantitative assessment.

The imaging mechanisms of MPI and CMR differ, reflecting myocardial injury from distinct perspectives. Using CMR as a reference, the MPI segment-level sensitivity of 84.1%, indicates good detection of CMR-identified abnormalities, while the low specificity (37.2%) and weak kappa values (0.13-0.19) reflect that MPI identifies perfusion defects in many segments CMR considers normal. This may be due to: 1) gastrointestinal activity and attenuation correction affecting inferior and anterior walls; 2) diffuse myocarditis predominantly involving the septal wall, reducing visual detection in other walls; 3) CMR false-negatives, as quantitative CMR methods partly address limitations of visual assessment [11, 13]; 4) MPI detecting cellular dysfunction and perfusion impairment that precede or exceed tissue changes detectable by CMR. The weak kappa values despite good positive agreement are explained by high prevalence of disease (most segments are abnormal), which leads to highly imbalanced 2 × 2 tables, yielding high chance agreement and low kappa even when proportional agreement is moderate.

Although most quantitative parameters showed correlations between modalities, overall correlations were modest, indicating each technique has strengths and limitations. Relying solely on CMR may underestimate inflammatory injury or yield false-negatives [11]. MPI may compensate by assessing perfusion impairment and myocardial cellular dysfunction.

This study has several limitations. First, FM diagnosis was based on clinical criteria without histopathological confirmation. Using CMR as a reference to evaluate MPI diagnostic performance also lacks histopathological support, introducing bias. Second, due to retrospective data collection, gated MPI acquisition was not performed in a proportion of patients, EF-MPI, and serological parameters were not available for all patients. Third, MPI and CMR were performed at different time points (median interval 1 day, IQR 1-2 days), and the evolving nature of FM may influence agreement which may not reflect the simultaneous cardiac status, although previous studies have suggested that the tissue repair process of FM myo-

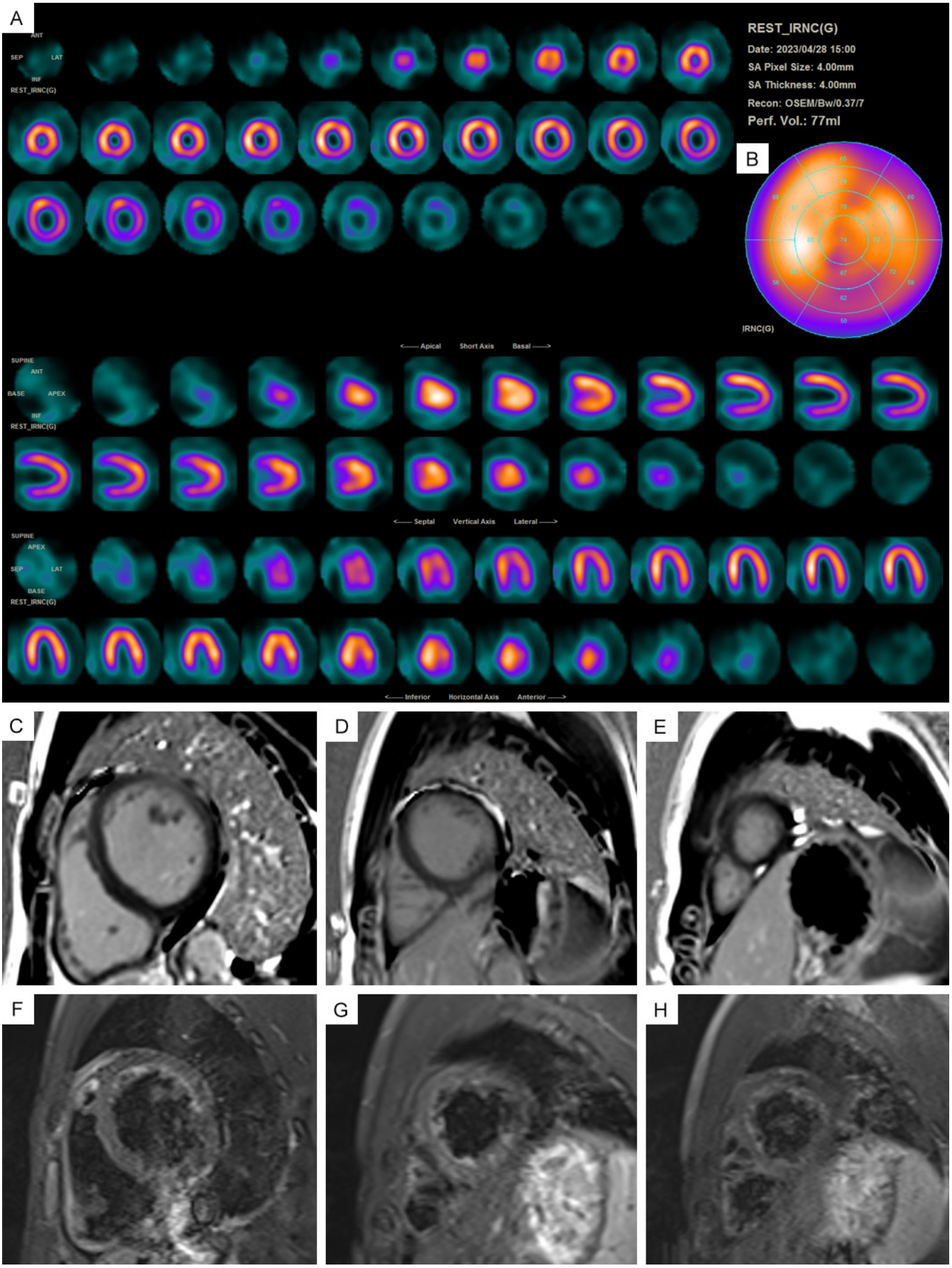


Figure 2. Representative case (male, 29 yo) with reduced perfusion on MPI and normal CMR. MPI demonstrated mild-to-moderate reduced uptake involving anterior, basal lateral wall, and inferior walls (A, B). CMR LGE (C-E) and T2-weighted (F-H) images showed no significant abnormalities.

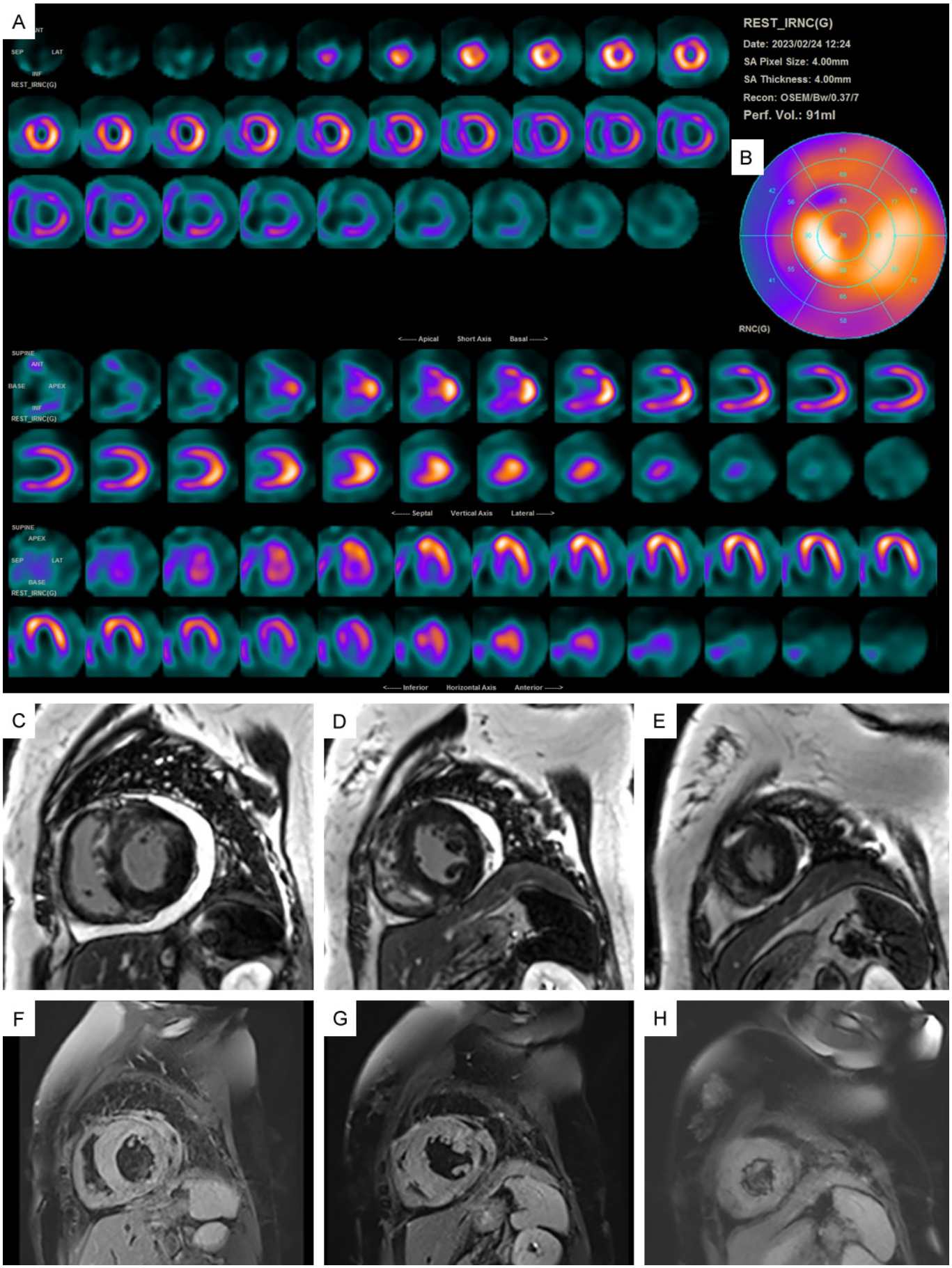

A
REST_IRNC(G)
Date: 2023/02/24 12:24
SA Pixel Size: 4.00mm
SA Thickness: 4.00mm
Recon: OSEM/Bw/0.37/7
Perf. Vol.: 91ml
B
RNC(G)
<------ Apical Short Axis Basal ------>
<------ Septal Vertical Axis Lateral ------>
<------ Inferior Horizontal Axis Anterior ------>
C
D
E
F
G
H

Figure 3. Representative case (female, 58 yo) with more extensive CMR involvement. MPI demonstrated extensive areas of mildly to severely reduced tracer uptake in anterior, adjacent anterolateral mid-to-basal inferior wall, and mid-to-basal septal walls (A, B). CMR T2-weighted images revealed diffuse patchy hyperintensity (F-H). LGE showed patchy/nodular enhancement in basal-to-mid septum, anterior and lateral walls, apical anteroseptal wall, and right ventricular septum (C-E).

Table 2. Wall segment level positive findings on MPI and CMR

Modality / Finding	MPI		CMR	
	Reduced perfusion	T2 hyperintensity	Reduced perfusion	LGE
Anterior	58	25	9	36
Septal	55	35	37	60
Lateral	61	30	11	47
Inferior	65	32	9	42
Total	239	122	66	185
Patients Involved (n = 77)	77	40	40	71

Table 3. Correlation of quantitative parameters between MPI and CMR or Laboratory data

Parameters	SRS (n = 77)		EF_MPI (n = 33)	
	r	*P*	*r*	*P*
T1	0.309**	0.006	-0.321	0.068
ECV	0.325**	0.004	-0.155	0.39
LGE	0.211	0.075	-0.373*	0.036
T2	0.219	0.056	-0.455**	0.008
EF_CMR	-0.421**	< 0.001	0.738**	< 0.001
NT-proBNP	0.306*	0.010	-0.251	0.182
WBC	0.075	0.518	-0.368*	0.035
Neutrophil	0.043	0.716	-0.202	0.261
Lymphocytes	0.298**	0.009	-0.388*	0.026
PCT	0.259	0.079	-0.519*	0.023

Note: *$P < 0.05$, **$P < 0.01$.

cardial injury usually lasts for weeks to months [6, 20]. Fourth, current technical limitations prevented image fusion, potentially causing segmental matching errors. Fifth, the lack of CMR-negative patients prevented patient-level specificity assessment. Sixth, patients with the most severe disease who could not tolerate CMR or who recovered rapidly may have been excluded, potentially limiting generalizability to the entire FM spectrum. Seventh, our segment-level analysis did not account for within-patient clustering; however, sensitivity analyses using generalized estimating equations produced consistent results, and we acknowledge this as a limitation. Eighth, multivariable regression was not performed due to sample size limitations, and future larger studies should explore independent predictors of MPI abnormalities.

In conclusion, MPI may serve as a complementary imaging modality for evaluating myocardial injury in FM, particularly when CMR is not feasible (e.g., unstable patients, gadolinium allergy, severe claustrophobia, or implantable cardioverter defibrillator devices, ICD). While our findings support complementarity, prospective studies with EMB and outcome data are needed to define the incremental prognostic value of MPI in FM management.

Acknowledgements

We acknowledge Dr. Yue Wu, Hong Li, Mr. Jie Zhang, Ms. Ying Zhang, and Ms. Li Liang for their invaluable assistance and academic guidance in this work.

Disclosure of conflict of interest

None.

Address correspondence to: Dr. Chengyan Dong, Department of Nuclear Medicine, First Hospital of Shanxi Medical University, Taiyuan, Shanxi, China. E-mail: drnickdong@qq.com; Dr. Jing Cui, Department of Nuclear Medicine, Fuwai Central China Cardiovascular Hospital, Zhengzhou, Henan, China. E-mail: Cuijj.zzu@163.com

References

[1] Hang W, Chen C, Seubert JM and Wang DW. Fulminant myocarditis: a comprehensive review from etiology to treatments and outcomes. Signal Transduct Target Ther 2020; 5: 287.

[2] Li S, Xu S, Li C, Ran X, Cui G, He M, Miao K, Zhao C, Yan J, Hui R, Zhou N, Wang Y, Jiang J, Zhang J and Wang D. A life support-based comprehensive treatment regimen dramatically lowers the in-hospital mortality of patients with fulminant myocarditis: a multiple center study. Sci China Life Sci 2019; 62: 369-380.

[3] Tschope C, Ammirati E, Bozkurt B, Caforio ALP, Cooper LT, Felix SB, Hare JM, Heidecker B, Heymans S, Hubner N, Kelle S, Klingel K, Maatz H, Parwani AS, Spillmann F, Starling RC, Tsutsui H, Seferovic P and Van Linthout S. Myocarditis and inflammatory cardiomyopathy: current evidence and future directions. Nat Rev Cardiol 2021; 18: 169-193.

[4] Jain A, Rane RP, Mumtaz M, Butt AY, Abdelsalam M and Waseem S. Fulminant coxsackievirus myocarditis in an immunocompetent adult: a case report and literature analysis. Cureus 2022; 14: e25787.

[5] Ammirati E, Cipriani M, Moro C, Raineri C, Pini D, Sormani P, Mantovani R, Varrenti M, Pedrotti P, Conca C, Mafrici A, Grosu A, Briguglia D, Guglielmetto S, Perego GB, Colombo S, Caico SI, Giannattasio C, Maestroni A, Carubelli V, Metra M, Lombardi C, Campodonico J, Agostoni P, Peretto G,

Scelsi L, Turco A, Di Tano G, Campana C, Belloni A, Morandi F, Mortara A, Cirò A, Senni M, Gavazzi A, Frigerio M, Oliva F and Camici PG; Registro Lombardo delle Miocarditi. Clinical presentation and outcome in a contemporary cohort of patients with acute myocarditis: multicenter lombardy registry. Circulation 2018; 138: 1088-1099.

[6] Chinese Society of Cardiology, Chinese Medical Association, Writing Group, Jiang J, Shu H, Wang DW, Hui R, Li C, Ran X, Wang H, Zhang J, Nie S, Cui G, Xiang D, Shao Q, Xu S, Zhou N, Li Y, Gao W, Chen Y, Bian Y, Wang G, Xia L, Wang Y, Zhao C, Zhang Z, Zhao Y, Wang J, Chen S, Jiang H, Chen J, Du X, Chen M, Sun Y, Li S, Ding H, Ma X, Zeng H, Lin L, Zhou S, Ma L, Tao L, Chen J, Zhou Y and Guo X. Chinese Society of Cardiology guidelines on the diagnosis and treatment of adult fulminant myocarditis. Sci China Life Sci 2024; 67: 913-939.

[7] Sawamura A, Okumura T, Ito M, Ozaki Y, Ohte N, Amano T and Murohara T; CHANGE PUMP Investigators. Prognostic value of electrocardiography in patients with fulminant myocarditis supported by percutaneous venoarterial extracorporeal membrane oxygenation - analysis from the CHANGE PUMP study. Circ J 2018; 82: 2089-2095.

[8] Kociol RD, Cooper LT, Fang JC, Moslehi J, Pang PS, Sabe MA, Shah RV, Sims DB, Thiene G and Vardeny O; American Heart Association Heart Failure and Transplantation Committee of the Council on Clinical Cardiology. Recognition and initial management of fulminant myocarditis: a scientific statement from the American heart association. Circulation 2020; 141: e69-e92.

[9] Sharma AN, Stultz JR, Bellamkonda N and Amsterdam EA. Fulminant myocarditis: epidemiology, pathogenesis, diagnosis, and management. Am J Cardiol 2019; 124: 1954-1960.

[10] Ammirati E, Veronese G, Bottiroli M, Wang DW, Cipriani M, Garascia A, Pedrotti P, Adler ED and Frigerio M. Update on acute myocarditis. Trends Cardiovasc Med 2021; 31: 370-379.

[11] Ferreira VM, Schulz-Menger J, Holmvang G, Kramer CM, Carbone I, Sechtem U, Kindermann I, Gutberlet M, Cooper LT, Liu P and Friedrich MG. Cardiovascular magnetic resonance in nonischemic myocardial inflammation: expert recommendations. J Am Coll Cardiol 2018; 72: 3158-3176.

[12] Germano G, Kavanagh PB, Slomka PJ, Van Kriekinge SD, Pollard G and Berman DS. Quantitation in gated perfusion SPECT imaging: the Cedars-Sinai approach. J Nucl Cardiol 2007; 14: 433-454.

[13] Cundari G, Galea N, De Rubeis G, Frustaci A, Cilia F, Mancuso G, Marchitelli L, Catapano F, Carbone I, Catalano C and Francone M. Use of the new Lake Louise Criteria improves CMR detection of atypical forms of acute myocarditis. Int J Cardiovasc Imaging 2021; 37: 1395-1404.

[14] Gottbrecht M, Kramer CM and Salerno M. Native T1 and extracellular volume measurements by cardiac MRI in healthy adults: a meta-analysis. Radiology 2018; 290: 317-326.

[15] Xu Z, Li W, Wang J, Wang F, Sun B, Xiang S, Luo X, Meng Y, Wang X, Wang X, Song J, Zhang M, Xu D, Zhou X, Ju Z, Sun J, Han Y and Chen Y. Reference ranges of myocardial T1 and T2 mapping in healthy Chinese adults: a multicenter 3T cardiovascular magnetic resonance study. J Cardiovasc Magn Reson 2023; 25: 64.

[16] Yang L, Li J, Zhang K, Zhao K, Liu Y, Luo Y, Huang L and Zhang X. Diagnostic efficacy of SPECT/CT MPI and CMR in children with myocarditis caused by different infection sources. Am J Nucl Med Mol Imaging 2022; 12: 180-187.

[17] Mansour N, Nekolla SG, Reyes E, Angelidis G, Georgoulias P, Anagnostopoulos C, Bravo P, Bruno I, Flotats A, Fuentes-Ocampo F, Sciagra R, Keng F, Kessler L, Papathanasiou M, Soman P and Rischpler C. Multi-center study of inter-rater reproducibility, image quality, and diagnostic accuracy of CZT versus conventional SPECT myocardial perfusion imaging. J Nucl Cardiol 2023; 30: 528-539.

[18] Liang STG, Mo L, Wei X, Huang M and Wang T. The clinical value of gated myocardial perfusion imaging in diagnosing suspected viralmyocarditis. J Qiqihar Med Univ 2014; 35: 1281-1282.

[19] Matsuo S, Nakajima K and Kinuya S. Evaluation of cardiac mitochondrial function by a nuclear imaging technique using technetium-99m-MIBI uptake kinetics. Asia Ocean J Nucl Med Biol 2013; 1: 39-43.

[20] Section of Precision Medical of Chinese Society of Cardiology of Chinese Medical Association; Editorial Board of Chinese Journal of Cardiology; Working Group on Adult Myocarditis. Chinese expert consensus statement on clinical diagnosis and treatment of fulminant myocarditis in adults. Zhonghua Xin Xue Guan Bing Za Zhi 2017; 45: 742-752.

[21] Chan N, Litwok Y, Boutis L and Makaryus JN. SPECT myocardial perfusion imaging findings in a patient with hypereosinophilic myocarditis. J Nucl Cardiol 2020; 27: 686-687.

[22] Javadi H, Jallalat S, Pourbehi G, Semnani S, Mogharrabi M, Nabipour I, Ravanbod M, Amini A and Assadi M. The role of gated myocardial perfusion scintigraphy (GMPS) in myocarditis: a case report and review of the literature. Nucl Med Rev Cent East Eur 2011; 14: 112-115.

[23] Xin K, Ma X, Meng X, Zhang X, Yang W, Ma T, Zhou C, Wang J and Li G. Assessment of myocardial injury by SPECT myocardial perfusion imaging in patients with COVID-19 infection in a single center after lifting the restrictions in China. Ann Nucl Med 2024; 38: 971-979.

[24] Laganà B, Schillaci O, Tubani L, Gentile R, Danieli R, Coviello R, Baratta L and Scopinaro F. Lupus carditis: evaluation with technetium-99m MIBI myocardial SPECT and heart rate variability. Angiology 1999; 50: 143-148.

[25] Norikane T, Mitamura K, Yamamoto Y, Takami Y, Fujimoto K, Noma T and Nishiyama Y. Immune checkpoint inhibitor myocarditis mimicking Takotsubo cardiomyopathy on MPI. J Nucl Cardiol 2022; 29: 2694-2698.